High Accuracy Measurement with 360° and Giga-pixel Panorama Images

Jafar Amiri Parian
FODIS, Hauptstr. 14, CH-8512 Lustdorf, Switzerland

Abstract

Panoramic cameras with Linear Array CCD have been originally built for purely imaging purposes, but they also have a high potential for use in high accuracy measurement applications. They have the advantage of high information content with giga-pixel format size and 360° field of view. Viewing 360° images is a natural way for the human being to perceive an environment. The ability to process data directly from 360° high resolution panorama RGB images makes the workflow extremely intuitive, natural and realistic. FODIS Measure3D is a combination of a fast panorama camera and innovative software packages for the extraction of 3D information from panoramic imagery. We present the sensor model for FODIS panorama camera and the results of self-calibration, which indicate a subpixel accuracy level. We demonstrate the systems' accuracy of 1mm in 10 meters in 3D point positioning, using a 3D testfield with a free network adjustment. With FODIS Measure3D we do have additional powerful sensors for image recording and efficient 3D object modeling.

1 Introduction

The word "panorama" is a combination of Greek terms, namely the suffix *pan* ($\pi\alpha\nu$), meaning "all", and *horama* ($o\rho\alpha\mu\alpha$), meaning "sight". In more technical terms, a panorama is defined as a picture or a series of pictures of a landscape, a historical event, etc. representing a continuous scene, enclosing the spectator and providing an unlimited view in all directions (synonymously the term "omnidirectional" is used). In both cases the meaning of a very wide field of view is conveyed.

The techniques of panorama production can be divided in two different groups (Fig. 1): catadioptric and dioptric systems. Dioptrics is the science of refracting elements (lenses) whereas catoptrics is the science of the reflecting surfaces (mirrors). The combination of refracting and reflecting elements is called catadioptrics. Catadioptric systems (Baker and Nayar, 1998; Svoboda et al., 1997; Ollis et al., 1999; Boult, 1998) use one or more mirrors with one or more cameras to capture a wide view angle of the scene. The images then need mosaicking and in special cases, seamless panoramas can be created. Planar and curved mirrors are used in these systems.

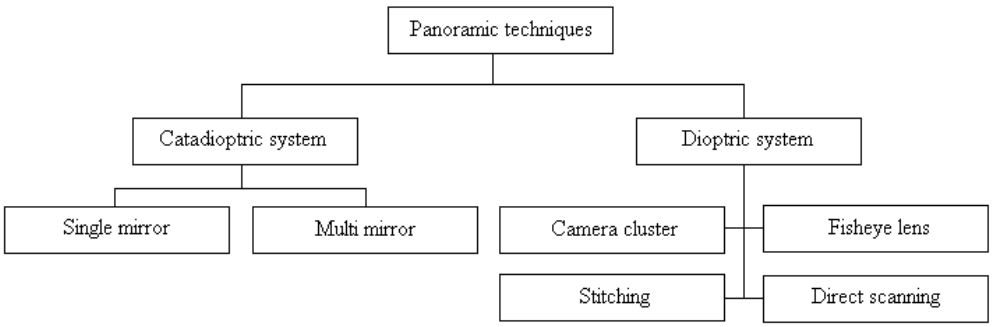

Fig. 1. Panoramic techniques. Subdivision into catadioptric and dioptric systems.

A dioptric system relates to its refractive elements (lenses). Mirrors may be included in these systems, but then the aim is to fold the optical system assembly and not increase the field of view. Dioptric systems are divided into four groups: camera cluster, fisheye lens, stitching and direct scanning. The first group uses several cameras, mounted on a surface and looking outwards onto the scene, which enables the capturing of the wide view (Nielsen, 2005). The second group consists of a camera with a fisheye lens which usually has more than 180° field of view (Herbert, 1987). They have been used in measurement applications (Colcord, 1989; Rich, 1990; Schwalbe, 2005; Heuvel et al., 2006). The third group produces a panoramic image by mosaicking or stitching the images (Shum and Szeliski, 1997). This technique has also been used in measurement applications

(Pöntinen, 1999; Petsa et al, 2001; Luhmann and Tecklenburg, 2002, 2004; Kukko, 2004; Heikkinen, 2005). The fourth group is related to a camera system with a rotating camera or rotating lens, which produces a seamless image without any need of stitching (Antipov and Kivaev, 1984; Hartley, 1993). A traditional terrestrial panoramic camera which operates by this method exposes a small portion of a film continuously at each specific time.

By using digital technology, digital rotating panoramic cameras were developed. Such camera system consists of a Linear Array which is mounted parallel to the rotation axis on a high precision turntable. By rotation of the turntable, the Linear Array sensor captures the scene as a continuous set of vertical scan lines.

FODIS Measure3D is a combination of a fast high resolution 360° panorama camera (Fig. 2) with innovative software packages, allowing direct 3D measurement in RGB images rapidly and accurately. The FODIS panorama camera has three parts: a camera head, an optical part, and a high precision motor. The camera head, which consists of a linear array of CCD, allows rapid image acquisition in Time Delay Integration (TDI) mode typically in few seconds for a 360° image capture. Camera control and image transfer to a tablet PC are performed via gigabit Ethernet. The optical part of the system allows the use of different lenses. The camera head is mounted on a high precision rotating motor. By rotation of the motor, the linear array sensor captures the scenery as a continuous set of vertical scan lines. Rotation speed and scanning angle are pre-selectable and correspond to the shutter speed, image size and the focal length of the lens. FODIS Measure3D software is a unique close range photogrammetry software capable of processing frame array and panoramic imagery. It includes advanced methods of camera calibration, image processing and optimization to assure high accuracy and reliability.

Fig. 2. FODIS panorama camera together with a tablet PC for camera control and image storage.

In this paper we present the mathematical sensor model for panoramic cameras. We show the results of self-calibration and accuracy testing. We also present the results of some applications.

2 Sensor Model for the Ideal Panoramic Camera

The sensor model as a mapping function is based on a perspective projection in the form of bundle equations, which maps the 3D object space points onto the Linear Array coordinate system. For the derivation of the equations four coordinate systems are defined:

- pixel coordinate system,
- Linear Array coordinate system,
- turntable coordinate system,
- 3D object coordinate system.

Fig. 3 shows the coordinate systems: pixel (i, j), Linear Array (0, y, z), turntable (X', Y', Z') and object space (X, Y, Z) coordinate systems. To define the turntable coordinate system, an ideal panoramic camera is assumed. The origin of the turntable coordinate system (O) coincides with the projection center. The rotation axis passes through the projection center and coincides with Z'. X' passes through the start position of the Linear Array before rotation and Y' is defined to get a right-handed coordinate system. Eq. (1), which is a 3D conformal

transformation with 6 parameters, shows the relation between the object space coordinate system and the turntable coordinate system:

$$\begin{pmatrix} X' \\ Y' \\ Z' \end{pmatrix} = M_{\omega,\varphi,k} \cdot \begin{pmatrix} X - X_0 \\ Y - Y_0 \\ Z - Z_0 \end{pmatrix} \tag{1}$$

with

(X_0, Y_0, Z_0) .... location of the origin of the turntable coordinate system in the object space coordinate system
(X, Y, Z) ..... object space coordinates
(X', Y', Z') ..... object point coordinates in the turntable coordinate system
$M_{\omega,\varphi,k}$ ..... rotation matrix with elements defined in Eq. (2).

$$M^{t}_{\omega,\varphi,\kappa} = R = \begin{bmatrix} \cos\varphi\cos k & -\cos\varphi\sin k & \sin\varphi \\ \cos\omega\sin k + \sin\omega\sin\varphi\cos k & \cos\omega\cos k - \sin\omega\sin\varphi\sin k & -\sin\omega\cos\varphi \\ \sin\omega\sin k - \cos\omega\sin\varphi\cos k & \sin\omega\cos k + \cos\omega\sin\varphi\sin k & \cos\omega\cos\varphi \end{bmatrix} \tag{2}$$

where ω, φ and κ are rotation angles of the turntable coordinates axes (X', Y', Z') with respect to the object space coordinates axes (X, Y, Z). The 6 parameters ($\omega, \varphi, \kappa, X_0, Y_0, Z_0$) of Eq. (1) define the "exterior orientation parameters" of a panoramic camera. Eq. (3) shows the relation of an image point in the Linear Array coordinate system with respect to an object point in the turntable coordinate system.

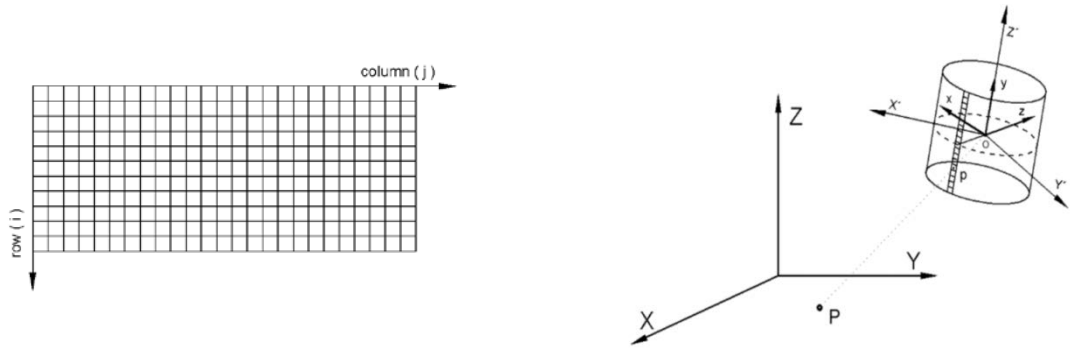

(a) (b)

Fig. 3. Object coordinate (X, Y, Z), turntable coordinate (X', Y', Z') and Linear Array (0, y, z) coordinate systems.

$$\begin{pmatrix} X' \\ Y' \\ Z' \end{pmatrix} = R^{t}_{Z'}(\theta) \cdot \lambda \cdot T \cdot \begin{pmatrix} 0 \\ y \\ -c \end{pmatrix} \tag{3}$$

with

$$y = (i - \frac{N}{2}) \cdot p_y, \quad \theta = j \cdot p_x, \quad T = \begin{pmatrix} 0 & 0 & -1 \\ -1 & 0 & 0 \\ 0 & 1 & 0 \end{pmatrix} \tag{4}$$

Where

p_x ..... angular pixel size of the turntable (rotation angle between two successive Linear Array image acquisitions)
p_y ..... pixel size of the Linear Array
c..... camera constant
N..... number of pixels in the Linear Array

$R_{Z'}$..... 3D rotation matrix around Z' axis
T..... transfer matrix from the Linear Array to the turntable coordinate system
$(0,y,-c)$ image point coordinates in the Linear Array coordinate system
(i, j)..... image point coordinates in the pixel coordinate system
λ ..... scale factor.

Finally the model which relates the image point coordinates (i, j) to the object point coordinates (X, Y, Z) becomes for an ideal sensor:

$$M_{w,\varphi,k} \cdot \begin{pmatrix} X - X_0 \\ Y - Y_0 \\ Z - Z_0 \end{pmatrix} = R^t_{Z'}(\theta) \cdot \lambda \cdot \begin{pmatrix} c \\ 0 \\ y \end{pmatrix} \tag{5}$$

with (θ, y) as shown in Eq. (4).

3 Systematic Errors and Additional Parameters of Panoramic Cameras

In practice a real panoramic camera deviates from the ideal one. These deviations, which are denoted as systematic errors, are modeled by additional parameters. The sources of systematic errors are: the lens, the configuration of the Linear Array with respect to the optical axis and the turntable rotation axis, and the turntable itself. The sources of some of the systematic errors of panoramic cameras are similar to the frame array CCD cameras. Therefore, the same additional parameters are used for the modeling. The other systematic errors, which can only be observed for panoramic cameras, are explored through the geometrical analysis of the sensor mechanical design and physical measurements of the errors. In addition, image point residuals are analyzed for a better understanding of the behavior of the systematic errors.

With respect to the stability of a panoramic camera, systematic errors can be divided into two different classes: stationary and non-stationary systematic errors. However, some of the parameters of one class might shift to the other class depending on the stability of the camera system. The aim of this classification is to enable the understanding of the sensor behavior and sensor modeling.

The systematic errors that are not varying with time are called stationary systematic errors. These errors remain constant in at least one epoch of data acquisition and over relatively long time (e.g. between two calibrations). The stationary systematic errors for panoramic cameras are divided into two groups as follow:

1. Errors only for panoramic cameras are
   - different scale factors for the two image axes, induced by errors of the angular pixel size
   - tilt and inclination of the Linear Array with respect to the rotation axis of the turntable
   - eccentricities of the projection center of the lens with respect to the rotation axis of the turntable and the origin of the turntable coordinate system.

2. Errors common between frame array CCD and panoramic cameras which are
   - lens distortions
   - shift of principal point
   - size of camera constant.

The second group of systematic errors is modeled by a sub-set of Brown's additional parameters (Brown, 1976). A new set of additional parameters is developed for the first group. Eq. (6) shows the integration of the new additional parameters into Eq. (5):

$$M_{w,\varphi,k} \cdot \begin{pmatrix} X - X_0 \\ Y - Y_0 \\ Z - Z_0 \end{pmatrix} = R^t_{Z'}(\theta - d\theta) \cdot \left(\lambda \cdot R_{Y'}(ly) \cdot R_{X'}(lx) \cdot \begin{pmatrix} c \\ 0 \\ y \end{pmatrix} + \begin{pmatrix} ex \\ ey \\ ez \end{pmatrix} \right) \tag{6}$$

with

$$d\theta = j \cdot dp_x \tag{7}$$

where

$R_{Y'}$, $R_{X'}$....	3D rotation matrices around *Y'* and *X'* axes of the turntable coordinate system
ex, ey, ez..	eccentricities of the projection center from the origin of the turntable coordinate axis
lx, ly.....	inclination and tilt of the Linear Array with respect to the turntable coordinate axis
dp_x.....	correction to the angular pixel size.

Fig. 4 shows the eccentricities of the projection center, tilt and inclination of the Linear Array with respect to the rotation axes. In practice, the height of the projection center (PC), *ez,* from the plane of the turntable is considered to be known and used as a constant parameter, because otherwise it would have a high correlation with Z_0 (exterior orientation parameter).

A sub-set of Brown's additional parameters (Brown, 1976) is used with some modification to model the radial symmetrical lens distortion, a correction to the camera constant and a shift of the principal point:

$$dy = dy_0 + \frac{\bar{y}}{c} \cdot dc + \bar{y}^3 \cdot (k_1 + k_2 \cdot \bar{y}^2) \tag{8}$$

with $\bar{y} = y - y_0$,

where

dy_0	correction to the shift of the principal point along Linear Array
k_1, k_2	parameters of radial symmetrical lens distortion
dc	correction to the camera constant.

Eq. (9) shows the integration of the Eq. (8) into Eq. (6).

$$M_{w,\varphi,k} \cdot \begin{pmatrix} X - X_0 \\ Y - Y_0 \\ Z - Z_0 \end{pmatrix} = R^t_{Z'}(\theta - d\theta) \cdot \left(\lambda \cdot R_{Y'}(ly) \cdot R_{X'}(lx) \cdot \begin{pmatrix} c \\ 0 \\ y - dy \end{pmatrix} + \begin{pmatrix} ex \\ ey \\ ez \end{pmatrix} \right) \tag{9}$$

For non-stationary systematic errors the reader is referred to Amiri Parian 2007 and Amiri Parian & Gruen 2010.

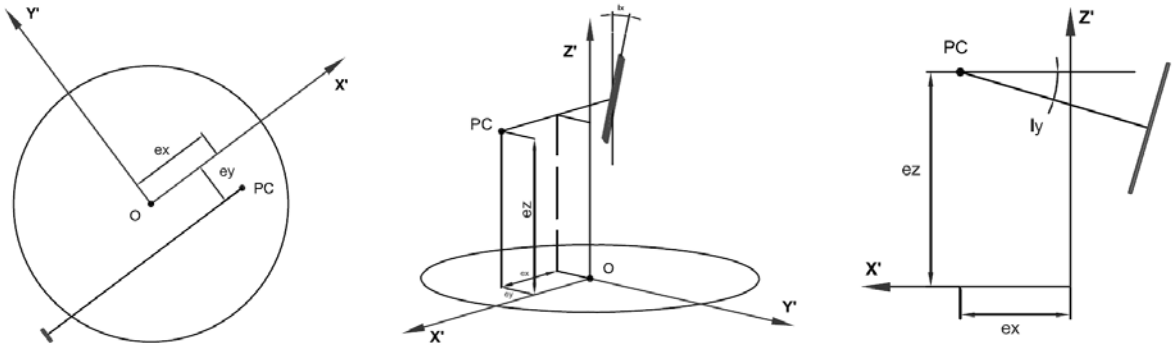

(a) (b) (c)

Fig. 4. Additional parameters for the configuration of the Linear Array with respect to the turntable coordinate system. (a) Eccentricities, (b) inclination of the Linear Array, (c) tilt of the Linear Array with respect to the rotation axis.

4 A Sensor Model with Additional Parameters for Panoramic Cameras

A sensor model with additional parameters is based on an observation equations model in which each single observation is expressed as an explicit function of unknown parameters.

In the first step, for the sake of simplicity, Eq. (3) is considered. From this equation, with the aim of constructing the functional model, Eq. (10) is constructed (Amiri Parian, 2007) as:

$$\begin{aligned} \theta &= -\tan^{-1}\left(\frac{Y'}{X'}\right) \\ y &= \frac{c \cdot Z'}{\sqrt{X'^2 + Y'^2}} \end{aligned} \tag{10}$$

The observation equations model of Eq. (9) is obtained similarly to Eq. (10). Eq. (11) shows this model after simplifications.

$$\begin{aligned} \theta &= -\tan^{-1}\left(\frac{\tilde{\tilde{Y}}}{\tilde{\tilde{X}}}\right) + d\theta \\ y &= \frac{c \cdot \tilde{\tilde{Z}}}{\sqrt{\tilde{\tilde{X}}^2 + \tilde{\tilde{Y}}^2}} + dy \end{aligned} \tag{11}$$

and with (θ, y) of Eq. (4):

$$\begin{pmatrix} \tilde{\tilde{X}} \\ \tilde{\tilde{Y}} \\ \tilde{\tilde{Z}} \end{pmatrix} = M_{w,\varphi,k} \cdot \begin{pmatrix} X - X_0 \\ Y - Y_0 \\ Z - Z_0 \end{pmatrix} - R^t_{Z'}(\theta) \cdot \begin{pmatrix} ex \\ ey \\ ez \end{pmatrix} \tag{12}$$

and

$$\begin{aligned} d\theta &= d\theta_{dc} + d\theta_{dy_0} + d\theta_{dp_x} + d\theta_{lx} + d\theta_{ly} + d\theta_{lens} + d\theta_{ex} + d\theta_{ey} \\ dy &= dy_{dc} + dy_{dy_0} + dy_{dp_x} + dy_{lx} + dy_{ly} + dy_{lens} + dy_{ex} + dy_{ey} \end{aligned} \tag{13}$$

Note that *ez* is a constant value and is equal to the height of the projection center from the turntable. The terms of Eq. (13) are expanded in Eqs. (14) and (15) according to

$$\begin{aligned} & d\theta_{dc} = d\theta_{dy_0} = d\theta_{ly} = d\theta_{lens} = d\theta_{ex} = d\theta_{ey} = 0 \\ & d\theta_{dp_x} = -j \cdot dp_x \\ & d\theta_{lx} = -\tan^{-1}\left(\frac{\bar{y}}{c} \cdot \sin(lx)\right) \end{aligned} \tag{14}$$

and

$$\begin{aligned} & dy_{dp_x} = dy_{\xi} = dy_{ex} = dy_{ey} = 0 \\ & dy_{dc} = \frac{\bar{y}}{c} \cdot dc \\ & dy_{dy_0} = y_0 + dy_0 \\ & dy_{lx} = \bar{y} \cdot \left(1 - \frac{c \cdot \cos(lx)}{\sqrt{c^2 + \bar{y}^2 \cdot \sin(lx)}}\right) \\ & dy_{ly} = \frac{\sin(ly) \cdot (\bar{y}^2 + c^2)}{c \cdot \cos(ly) + \bar{y} \cdot \sin(ly)} \\ & dy_{lens} = \bar{y}^3 \cdot (k_1 + k_2 \cdot \bar{y}^2) \end{aligned} \tag{15}$$

5 Sensor Self-Calibration and Accuracy Tests

The camera calibration was performed through self-calibration using the mathematical model developed in the previous section. The self-calibration was performed with block triangulation. This section reports the result of FODIS panoramic camera calibration through self-calibration.

5.1 Panoramic Testfield of Control Points

FODIS panoramic testfield of control points with a 360° horizontal field of view were used for self-calibration and accuracy testing. The control points are the coded targets. The bases of targets are white and the contrasts are black. FODIS panoramic testfield consists of more than 500 control points which have been measured with an independent measurement. The point positioning accuracy of the testfield is in average 0.5mm.

5.2 Results of Camera calibration and Accuracy Tests

The goal is to do the calibration and accuracy testing of the entire FODIS system. Several panorama images were acquired from this testfield. Fig. 5 shows the typical configuration of the camera stations for camera calibration. Image and photogrammetric processing were performed with FODIS Measure3D software. Photogrammetric computations were performed with the free network adjustment. The free network adjustment computes the overall geometry of the network by processing only the measurements. It needs at least one known distance between two points for scale the network of measurement. In these cases, scale was recovered from the size of coded targets.

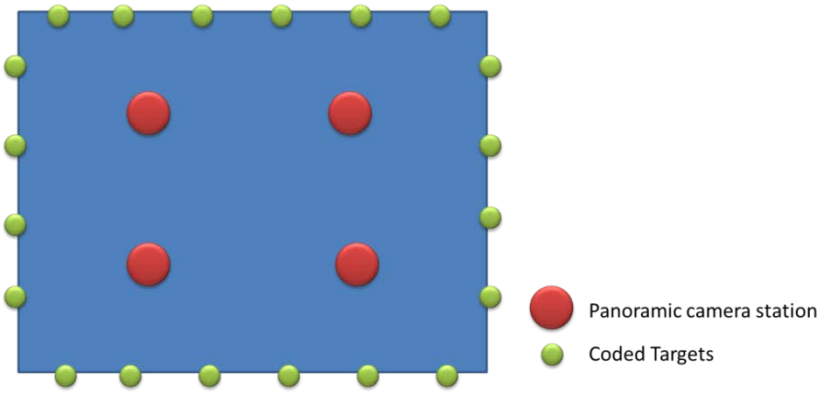

Fig. 5. A typical camera stations for panoramic camera calibration.

As the results the RMS of the image point residuals is **0.25 pixel** and **0.19 pixel** along column and row axes. The RMS error of positioning at check points is **0.7 mm** projecting it at distance of 10 meters it would be equal to 1 mm accuracy.

6 Applications

In the field of surveying and mapping, accuracy and reliability of measurement tools are key to success. A new system needs validation and testing under real environmental conditions. To this end, the FODIS system was tested in the field, comparing its workflow, productivity and accuracy to established measurement systems such as total stations and laser scanners.

Under the leadership of the Japanese Association of Surveyors, the new FODIS Measure3D system was benchmarked with a total station and a single-frame camera. One test was performed outdoor for accuracy and two tests indoor for productivity and system performance. The FODIS Measure3D system proved to be a viable and accurate alternative to total stations, especially in situations where the object to be measured can be viewed from different perspectives. With regards to productivity (time spent in the field and in the office) and in automatic data acquisition/storage, FODIS Measure3D has clear benefits (Amiri Parian, 2012).

In another practical project the FODIS system measured the dimensions of glass domes at Zurich's Botanical Gardens. This indoor assignment proved to be challenging for other mapping instruments because of many reflections, caused by the glass and metal structure, and occlusions due to the confined interior. To deal with

this complex environment more effectively, FODIS coded targets were attached to the dome structure, thus allowing automated image orientation and maximum accuracy for the final 3D measurements. Here again, the FODIS Measure3D solution set a new benchmark in productivity, as the 3D project was finished in less than a day (Fig. 6). For more information please see www.fodis.com.

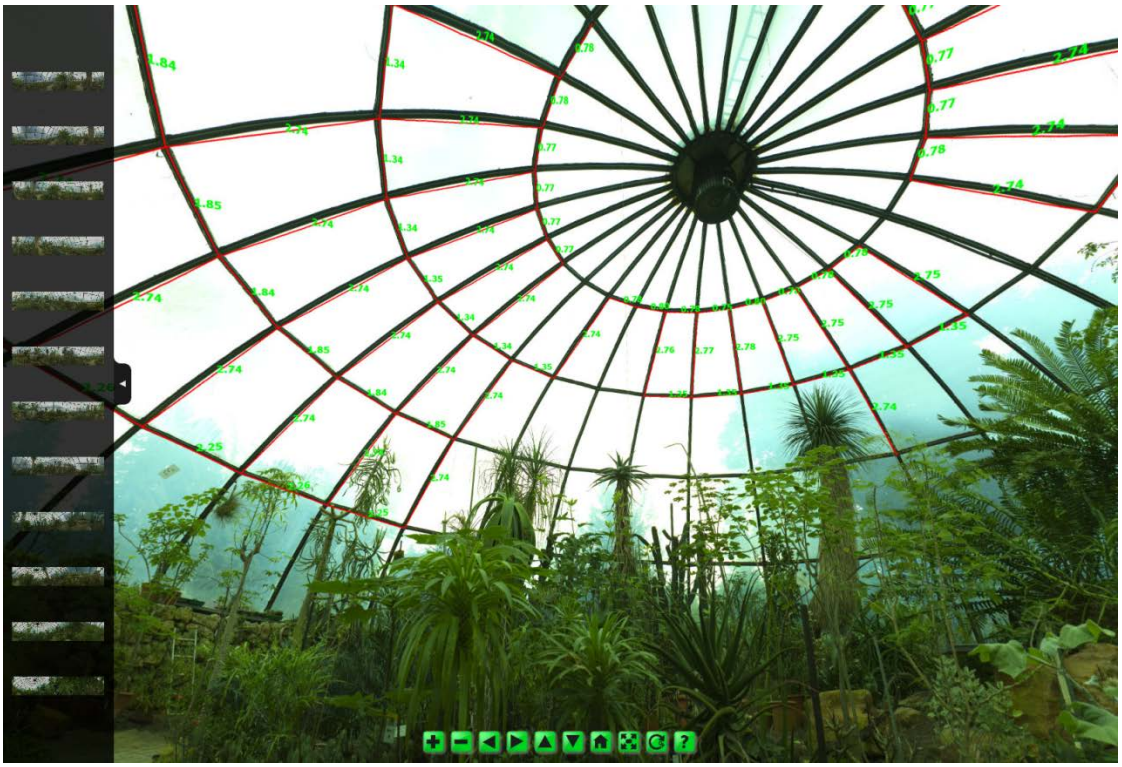

Fig. 6. 3D measurement and documentation with FODIS Measure3D of the Botanical Garden of Zurich.

7 Conclusions

FODIS Measure3D is a strong alternative especially for indoor measurements where rapid, accurate and selective point measurements are required. Furthermore, because the FODIS system provides a panoramic view and rich information content in resolution, it deals with complexity more efficiently than other measurement tools. At the same time, the FODIS system has the advantage of the image with embedded measurements, which allows easy sharing and visualization of results on new media such as intranet and the web. It is an accurate tool with 1mm in 10meters accuracy.

References

Amiri Parian, J., 2007. Sensor Modeling, Camera Calibration and Point Positioning with Terrestrial Panoramic Cameras. PhD dissertation, ETH No. 17094.

Amiri Parian, J., Gruen, A., 2010. Sensor Modeling, Self-Calibration and Accuracy Testing of Panoramic Cameras and Laser Scanners. ISPRS Journal of Photogrammetry and Remote Sensing, 65(1), January 2010, pp. 60-76.

Amiri Parian, J., 2012. Panorama Photogrammetry: Accurate 3D Documentation with High Resolution 360° Panoramic Images, GIM International Magazine, February 2012.

Antipov, I. T., Kivaev A. I., 1984. Panoramic Photographs in Close Range Photogrammetry. International Archives of Photogrammetry and Remote Sensing, XXV(A5), Comission V, pp. 32-38.

Baker, S., Nayar, S. K., 1998. A Theory of Catadioptric Image Formation. IEEE Proceedings of ICCV, pp. 35-42.

Boult, T. 1998. Remote reality via omnidirectional imaging. Proceedings of DARPA Image Understanding Workshop.

Brown, D.C., 1976. The bundle adjustment – progress and prospects. International Archive of Photogrammetry, Helsinki, Finland, 21(B3), 33 p.

Colcord, J.E., 1989. Using Fish-Eye Lens for GPS Site Reconnaissance. Journal of Surveying Engineering, 115(3), 347-352.

Hartley, R., 1993. Photogrammetric Techniques for Panoramic Camera. SPIE Proceedings, Vol. 1944, Integrating Photogram- metric Techniques with Scene Analysis and Machine Vision. Orlando, USA, pp. 127-139.

Heikkinen, J., 2005. The Circular Imaging Block in Close-Range Photogrammetry. Institute of Photogrammetry and Remote Sensing, Helsinki University of Technology, Doctoral Dissertation.

Herbert, T.J., 1987. Area Projections of Fisheye Photographic Lenses. Agricultural and Forest Metrology (39), 215-223.

Heuvel, F.A. van den, Verwaal, R. and Beers, B., 2006. Calibration of Fisheye Camera Systems and the Reduction of Chromatic Aberration. International Archives of Photogrammetry and Remote Sensing, 36(5), Dresden, Germany, 6 p. (on CD ROM).

Kukko, A., 2004. A New Method for Perspective Centre Alignment for Spherical Panoramic Imaging, The Photogrammetric Journal of Finland, 19(1), 37-46.

Luhmann, T., Tecklenburg, W., 2002. Bundle Orientation and 3-D Object Reconstruction from Multiple-Station Panoramic Imagery. International Archives of Photogrammetry and Remote Sensing, 34(5), Corfu, Greece, pp. 181-186.

Luhmann, T., Tecklenburg, W., 2004. 3-D Object Reconstruction from Multiple-Station Panorama Imagery. International Archives of Photogrammetry and Remote Sensing, 34(5/W16), 8 p. (on CDROM).

Nielsen, F., 2005. Surround video: a multihead camera approach. The visual computer, 21(1-2), 92-103

Ollis, M., Herman, H. and Singh, S., 1999. Analysis and Design of Panoramic Stereo Vision Using Equi-Angular Pixel Cameras. The Robotics Institute Carnegie Mellon University, CMU-RI-TR-99-04, Pittsburgh, PA 15213, 43 p.

Petsa, E., Kouroupis, S. and Karras, G.E., 2001. Inserting the past in video sequences. International Archives of Photogrammetry and Remote Sensing, 34(5C7), pp. 707-712.

Pöntinen, P., 1999. On the Creation of Panoramic Images from Image Sequences, Photogrammetric Journal of Finland, 16(2), 43-67.

Rich, P.M., 1990. Characterizing Plant Canopies with hemispherical Photographs. Remote Sensing Reviews, 5(1), 13-29.

Schwalbe, E., 2005. Geometric modeling and calibration of fisheye lens camera systems. International Archives of Photogrammetry and Remote Sensing, 36(5/W8), 6 p. (on CDROM).

Shum, H., Szeliski, R., 1997. Panoramic Image Mosaics. Microsoft Research, Technical Report, MSR-TR-97-23, 50 p.

Svoboda, T., Pajdla, T. and Hlavac, V., 1997. Central Panoramic Cameras: Geometry and Design. Research report K335/97/147, Czech Technical University, Faculty of Electrical Engineering, Center for Machine Perception, 16 p.